Density of States–Based Molecular Simulations

Sadanand Singh, Manan Chopra, and Juan J. de Pablo

Department of Chemical and Biological Engineering, University of Wisconsin, Madison, Wisconsin 53706; email: depablo@engr.wisc.edu

Annu. Rev. Chem. Biomol. Eng. 2012. 3:369–94

First published online as a Review in Advance on April 5, 2012

The *Annual Review of Chemical and Biomolecular Engineering* is online at chembioeng.annualreviews.org

This article's doi: 10.1146/annurev-chembioeng-062011-081032

1947-5438/12/0715-0369$20.00

Keywords

uniform sampling, metadynamics, flat histogram, flux maximization

Abstract

One of the central problems in statistical mechanics is that of finding the density of states of a system. Knowledge of the density of states of a system is equivalent to knowledge of its fundamental equation, from which all thermodynamic quantities can be obtained. Over the past several years molecular simulations have made considerable strides in their ability to determine the density of states of complex fluids and materials. In this review we discuss some of the more promising approaches proposed in the recent literature along with their advantages and limitations.

1. INTRODUCTION

Molecular simulations can be classified into two categories: Monte Carlo approaches (1), which seek to sample the configuration space of a system, and molecular dynamics (2, 3), which follow a system's evolution in time by integrating Newton's equation of motion. In either case, mechanical properties such as the internal energy U or the pressure P can be easily determined as direct averages of instantaneous properties such as the interactions between particles or the forces between them. Thermal properties, such as the free energy or the entropy, are more difficult to calculate. They cannot be extracted directly from a simulation and require that ensemble or time averages of indirect properties be determined (4). In the so-called Widom particle insertion approach (5), for example, one attempts to determine the average energy that a ghost particle would experience if it were inserted at random into the system of interest without disturbing the configuration of the existing, real particles. The average of the exponential of that energy is proportional to the chemical potential (or molar Gibbs free energy) of the system.

In recent years, however, molecular simulations have undergone a paradigm shift in which the free energy itself is used to guide sampling of the configuration space (6–50). Such methods not only offer the promise of more efficient sampling, particularly in systems characterized by rough free energy landscapes, but also lead to direct estimates of the free energy. This review focuses on a discussion of such methods, which we refer to collectively as density-of-states (DOS) sampling techniques.

A common problem encountered in molecular simulations is that of rare events. The free energy surfaces of complex systems, along predefined sets of coarse-grained variables or order parameters, often exhibit deep minima, corresponding to stable phases or states, separated by large barriers. Such barriers constitute sampling or dynamical bottlenecks that hinder the evolution of the system from one minimum to the next. The presence of free energy barriers and bottlenecks leads to a separation of timescales in which the time t spent in a stable state (basin of the free energy) is much greater than the time spent crossing the barriers. This separation of timescales serves to define a rare event—an event so infrequent that it defies study by traditional simulations (48). In DOS simulations, such a separation in timescales is countered by introduction of a biasing potential or force in the system that makes those two timescales commensurate. We begin this review with a brief overview of various DOS-based methods. Subsequent sections are devoted to a discussion of novel, more advanced algorithms that combine elements from multiple advanced sampling techniques. A **Supplemental Text** section describes the mathematical foundations of DOS methods (follow the **Supplemental Material link** from the Annual Reviews home page at **http://www.annualreviews.org**). A concluding section is devoted to a discussion of the general applicability of such techniques for simulations of complex systems in the areas of materials and biomolecular research.

2. DENSITY OF STATES SIMULATIONS

The central quantity of interest in DOS-based simulations is the microcanonical partition function or DOS $\Omega(E, V, N)$. For a given system with a volume V and number of particles N, Ω is proportional to the number of distinct states having energy E. All thermodynamic properties of the system can be calculated from knowledge of $\Omega(E, V, N)$. For example, the canonical ensemble average of a quantity $X(E)$ can be determined from $\Omega(E)$ according to

$$<X>_{NVT} = \frac{\sum_E X(E)\Omega(E)\mathrm{e}^{-\beta E}}{\sum_E \Omega(E)\mathrm{e}^{-\beta E}}, \qquad 1.$$

where the sum extends over the entire range of energy accessible to the system. Conventional canonical ensemble Monte Carlo or molecular dynamics simulations generate configurations that are distributed with probability proportional to $\Omega(E, V, N)\exp(-\beta E)$, where $\beta = 1/k_B T$, but do not yield a direct estimate of Ω. DOS methods provide a means to measure Ω directly.

A little over a decade ago, Wang & Landau (25) introduced a remarkably simple and effective approach for direct calculation of the DOS from a Monte Carlo simulation. Although several methods had already been proposed to estimate Ω, Wang & Landau's contribution was seminal in that it allowed for the automatic, on-the-fly calculation of the DOS of a system with little intervention from the user. Equally importantly, in their approach DOS guided the sampling, thereby allowing the method to overcome large free energy barriers in a systematic manner. The Wang-Landau (WL) method is based on the observation that if the configuration space is sampled according to a probability proportional to the reciprocal of the DOS, $\frac{1}{\Omega(E)}$, then the corresponding histogram of energies should be perfectly flat. In practice, a WL simulation is implemented by modifying an estimated DOS in a manner that produces a flat histogram of visits to distinct energy levels over a specified energy range. One starts with a simple guess of the DOS (e.g., $\Omega = 1$ for all values of E). A random walk in energy space is performed by generating trial configurations by simple random displacements; a trial configuration is accepted according to

$$p(E_1 \rightarrow E_2) = \min\left[\frac{\Omega(E_1)}{\Omega(E_2)}, 1\right], \qquad 2.$$

where E_1 and E_2 denote the energies of the system before and after the trial move. Every time that an energy level E is visited, the corresponding DOS is updated by multiplying the current value by a modification factor f that is greater than unity, i.e., $\Omega(E) \rightarrow \Omega(E) \times f$. The initial value f_0 of the modification factor can be set to $f_0 = e$. Such a choice allows for relatively fast sampling of all possible energy levels. A histogram of energy, $H(E)$, is also updated every time that an energy state is visited. The energy range of interest is sampled, and the DOS is modified until the accumulated histogram $H(E)$ becomes sufficiently flat. Sufficient flatness is achieved, for example, when all entries (or bins) of the histogram do not deviate by more than 70% or 80% from their mean, $\langle H(E)\rangle$. Once the histogram is flat, the modification factor is reduced according to the formula $f_1 = \sqrt{f_0}$, and the histogram $H(E)$ is reset to zero. The above cycle is repeated until the newly constructed histogram $H(E)$ is again flat. The algorithm stops when the modification factor f is smaller than a predefined value, typically in the vicinity of $\ln f = 10^{-10}$.

2.1. Multidimensional Density of States

The original WL DOS algorithm (25) was conceived in the context of an Ising system, which has discrete energy states. Yan et al. (49) and Faller et al. (50) subsequently extended that approach to systems in a continuum (a Lennard-Jones fluid). Yan et al. (49) also presented extensions to open systems in which both the number of particles N and the energy E were sampled for a Lennard-Jones fluid, thereby generating an estimate for $\Omega(N, E)$ over a wide range of density that enabled calculation of the entire phase behavior of the Lennard-Jones fluid. **Figure 1** shows the DOS $\Omega(N, E)$ of a Lennard-Jones system with the corresponding liquid-vapor coexistence curve. As shown in the figure, DOS simulations permit calculation of vapor-liquid equilibria at relatively low temperatures at which alternative approaches such as Gibbs ensemble simulations would be overly demanding. Subsequent refinements of the WL DOS algorithm facilitated applications to more complex systems (32, 51–57), including glasses (58), polymers (59), and proteins (60–65). In the following we discuss in more detail several extensions or refinements of the WL DOS method.

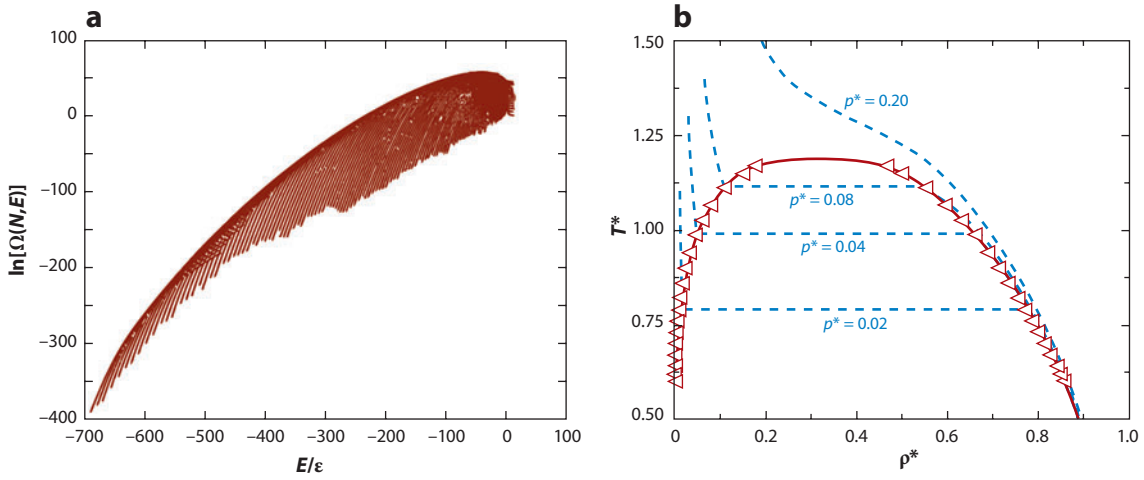

Figure 1

(*a*) Two-dimensional density of states and (*b*) the corresponding vapor-liquid coexistence curve for the truncated Lennard-Jones system. Each line in panel *a* corresponds to a different value of N in the range $N = 0$ to $N = 110$ for a volume of 125 σ^3 Lennard-Jones units. ρ^* represents the number density, p^* represents the pressure in reduced units, and T^* represents the temperature in reduced units. Reprinted with permission from Reference 49. Copyright © 2002, American Institute of Physics.

In cases in which it is of interest to determine the DOS as a function of E and V, regular canonical-ensemble displacement moves, in which trial configurations are generated through random perturbations of an existing configuration, must be supplemented with isobaric-ensemble volume moves, in which the volume of the simulation box is also changed. Canonical-ensemble trial moves (1) are accepted with the probability criteria given by Equation 2. Volume-change trial moves are accepted according to

$$P(E_1, V_1 \rightarrow E_2, V_2) = \min\left[1, \left(\frac{V_2}{V_1}\right)^N \frac{\Omega(E_1, V_1)}{\Omega(E_2, V_2)}\right]. \qquad 3.$$

Simulations are carried out in a manner analogous to that employed for 1D DOS; the $H(E, V)$ histogram is reset whenever it is deemed sufficiently flat, and the modification factor is decreased according to the prescription $f_{i+1} = \sqrt{f_i}$.

2.2. Expanded Ensemble Density of States

As outlined above, DOS algorithms can be used to generate different projections of the microcanonical DOS $\Omega(E, V, N)$, which can then be used to determine averages in traditional statistical mechanical ensembles such as the NVT, NPT, or μVT. There are cases, however, in which it is of interest to generate a free energy profile along a particular order parameter or reaction coordinate. Consider, for example, the potential of mean force that is required to bring two molecules in a liquid into close proximity. That potential of mean force is proportional to the radial distribution function and can be measured experimentally. Consider the potential of mean force required to unfold a protein by pulling on its ends, which can also be measured by atomic force microscopy. A potential of mean force can be determined by resorting to an expanded ensemble formalism (27, 28). The thermodynamic space of interest is subdivided into M states along an order parameter or reaction coordinate s such that the m^{th} state corresponds to a particular value of $s = s_m$. The

partition function of this expanded ensemble is given by

$$\Xi = \sum_{m=1}^{M} Q(N, V, T, m) w_m = \sum_{m=1}^{M} Q_m w_m, \quad 4.$$

where Q_m and w_m denote a canonical partition function and a positive weight factor for state m, respectively. The probability p_m with which a state m is visited is related to the partition function, Ξ, through

$$p_m = \frac{Q_m w_m}{\Xi}. \quad 5.$$

In general, one has the following relation between any two expanded states m and k:

$$\frac{Q_m}{Q_k} = \frac{p_m w_k}{p_k w_m}. \quad 6.$$

The free energy difference between two states m and k is therefore given by:

$$\beta[F(s_m) - F(s_k)] = -\ln \frac{Q_m}{Q_k} = -[\ln w_k - \ln w_m] + [\ln p_k - \ln p_m]. \quad 7.$$

If a uniform sampling of states is enforced, then $\ln p_k - \ln p_m = 0$ and $\beta[F(s_m) - F(s_k)] = -[\ln w_k - \ln w_m]$.

For a continuous order parameter, a uniform sampling of states can be achieved by performing DOS simulations along a reaction coordinate as opposed to energy space. This approach is referred to as expanded ensemble DOS (EXEDOS) (27, 28). The aim of the simulation is to determine the weights as a function of the order parameter, $w(s)$. One generates trial configurations through random displacements of the reaction coordinate and by accepting them according to

$$P(s_1 \rightarrow s_2) = \min[1, e^{-\beta(E_2 - E_1) - (\ln w_2 - \ln w_1)}]. \quad 8.$$

As before, $w(s)$ is initially assumed to be a constant, typically 1. A histogram $H(s)$ is accumulated and eventually reset to zero whenever it is deemed to be sufficiently flat. A modification factor is used to update $w(s)$, whose value is decreased as repeated cycles of the algorithm are performed. The converged value of $w(s)$ corresponds to the free energy profile along the reaction coordinate s, as indicated in Equation 7. The above formulation of EXEDOS can be further generalized to any number of dimensions, and can therefore be used to obtain free energy surfaces along an arbitrary number of order parameters.

2.3. Density of States with Molecular Dynamics: Metadynamics

The DOS and EXEDOS algorithms described above are based on Monte Carlo algorithms. Given the widespread availability of molecular dynamics simulation codes (66–71), however, it is of interest to devise advanced sampling techniques that rely on molecular dynamics moves to explore phase space. The central idea behind DOS simulations is to arrive at a set of weights (the DOS) such that sampling along a given thermodynamic variable or order parameter is uniform. That idea can be carried over to molecular dynamics techniques, in which properly chosen forces can be introduced to evolve the system in a manner that leads to uniform sampling. The so-called local elevation search method (14), various adaptive bias force methods (14, 24, 39–41, 44), and the self-healing umbrella sampling (72) technique are all examples of such a strategy.

Metadynamics, originally introduced by Parrinello and colleagues (73, 74), relies on similar ideas. In metadynamics, uniform sampling is sought along a finite number of collective variables (CVs), $s_\alpha(\mathbf{x})$, $\alpha = 1, 2, \ldots, d$, where d is a small number and $\mathbf{x}$ denotes the Cartesian coordinates

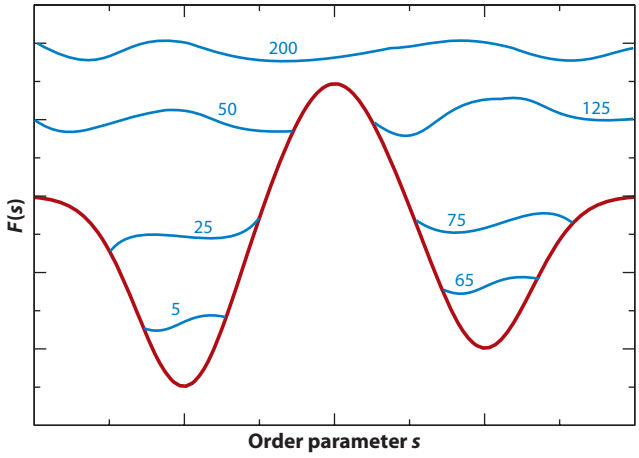

Figure 2

A schematic representation of the evaluation of potential energy, $F(s)$ in the metadynamics method along an order parameter s. The thick red line represents the bare potential energy $V(x)$ of the system. The thin blue lines correspond to the sum $V(x) + \sum V_G(x, t)$ at time t (see Equation 10). The numbers denote how many Gaussians have been added to the system at a given time t. As more and more Gaussians are added, the potential energy minima are gradually filled, and sampling of different states becomes increasingly uniform.

of the system. In a traditional molecular dynamics simulation, the system can be trapped in local energy minima. To promote uniform sampling, at intervals of time τ_G, metadynamics adds a small repulsive Gaussian potential to the system to help it escape from such minima. The height W and the width δs_α of the Gaussian potential are chosen to provide a reasonable compromise between accuracy and efficiency when exploring the free energy surface. At any given time t, for a system at a point $\mathbf{s}$ in CV space, the net force acting on all particles, $\mathbf{f}_{total}(t)$, is given by

$$\mathbf{f}_{total}(t) = -\frac{\partial V(\mathbf{x})}{\partial \mathbf{x}} - \sum_{\alpha=1}^{d} \frac{\partial V_G[s_\alpha(\mathbf{x}), t]}{\partial s_\alpha} \frac{\partial s_\alpha}{\partial \mathbf{x}}, \qquad 9.$$

where $V(\mathbf{x}, t)$ is the original potential energy at $\mathbf{x}$, and $V_G[s_\alpha(\mathbf{x}), t]$ is the net added Gaussian potential given by:

$$V_G(\mathbf{s}, t) = W \sum_{t' \leq t} \exp\left\{ -\sum_{\alpha=1}^{d} \frac{[s_\alpha - s_\alpha(t')]^2}{2\delta s_\alpha^2} \right\}. \qquad 10.$$

Figure 2 illustrates the mechanism by which hills are added to the actual potential energy. In addition to facilitating uniform sampling of the CV space, metadynamics also yields the free energy profile along the CVs according to $F(\mathbf{s}) = -V_G(\mathbf{s}, t \to \infty)$. Laio & Gervasio (75) recently published an extensive review of metadynamics.

One shortcoming of the original metadynamics prescription is that it does not offer a well-defined, optimal procedure to determine whether a simulation has converged. Several solutions have been proposed to address this issue, some of which are discussed in more detail in Section 4. One that stands out in the context of this review is that proposed by Min et al. (76), which takes advantage of a direct relationship between metadynamics (73, 74) and the WL DOS algorithm (25). In their implementation of metadynamics, the simulation is started with an arbitrary hill height W, and a histogram of visits to distinct collective variable states is recorded. Similar to the WL algorithm, once the histogram is sufficiently flat, W is decreased. The process continues until

the hills' height reaches some prespecified value. Additional details of this method are given in Section 4.1.

At this point it is instructive to emphasize the connection between WL DOS simulations (25), EXEDOS simulations (27), and metadynamics simulations (73). In an EXEDOS simulation with applied weights $w(s)$, the system is distributed along an order parameter s, $n_w(s) \propto w(s)\Omega(s)$, where $\Omega(s)$ is the DOS of the system. As discussed earlier, the goal of DOS simulations is to visit all states uniformly by constructing weights such that $w(s) \propto \frac{1}{\Omega(s)}$. Once converged, an EXEDOS simulation yields the free energy as $\beta F(s) = \ln w(s) = -\ln \Omega(s)$. In metadynamics, $F(s)$ is given by $-V_G(s)$, i.e., the negative of the sum of all of the added Gaussians, in the limit of long simulation times. The weights applied in a DOS simulation, $\ln w(s)$, are therefore equivalent to those applied in metadynamics, i.e., $F(s) = -V_G(s) = k_B T \ln w(s)$. In view of this relationship, it is of interest to discuss WL-based simulations and metadynamics approaches within the common umbrella of DOS, in which the central idea is for the underlying free energy surface to guide the simulation.

2.4. Convergence of Density of States–Based Methods

The mathematical foundations of DOS-based approaches are discussed in the Supplemental Text. Here we limit our discussion to the issue of convergence, which plays a central role in the accuracy and validity of a DOS-based simulation. The acceptance criteria in DOS algorithms are based on the on-the-fly estimation of Ω. This leads to a coupling of accepted states and the past history of the simulation. Therefore, unlike the case with regular Metropolis sampling (77), a DOS simulation does not follow a Markov process (46, 78, 79). Earl & Deem (80) have derived a general condition for convergence in Monte Carlo methods whose history dependence is contained in the simulated density distribution. The authors conclude that for a DOS method to converge, the condition of detailed balance need only be satisfied asymptotically, and the calculated DOS need only approach the exact DOS with an error proportional to the inverse of time. Several authors have examined the convergence of the DOS algorithm. Yan & de Pablo (81) were the first to realize that the original WL DOS approach reaches an asymptotic estimate of the density of states that does not improve with additional simulation time, and they proposed several strategies based on derivatives of Ω to overcome that problem (see Section 3.2). Zhou & Bhatt (79) showed analytically that for a model with N discrete energy states, the WL DOS algorithm does converge to the correct DOS Ω. They also found that the statistical error scales as $\sqrt{\ln f}$, where f is the modification factor. Lee et al. (82) also found this result in their simulations. Zhou & Bhatt (79) pointed out that the statistical error in DOS simulations can be decreased either by reducing f or by running multiple calculations. They showed that using large values of f leads to systematic errors in the calculated value of Ω owing to the correlation between adjacent records in the histograms. They proposed that DOS simulations be started with a large f and that f subsequently be reduced in large steps. Multiple measurements can then be made in the final stage to reduce the statistical error effectively.

Morozov & Lin (78) examined the accuracy and convergence of the DOS algorithm for a two-level system. Consistent with Zhou & Bhatt (79), they found that the statistical error scales as $\sqrt{\ln f}$. Furthermore, they found that the gradient of entropy S, $S = \ln \Omega$, also affects the accuracy and convergence of DOS methods. Given the dependence of convergence on the modification factor f, Belardinelli & Pereyra (83) proposed a time-dependent modification factor, namely, $f(t) \propto 1/t$. With that prescription, the calculated DOS $\Omega_{calc}(E, t)$ approaches asymptotically the exact value $\Omega_{exact}(E)$ as $\propto t^{-0.5}$, thereby avoiding the saturation error originally identified by Yan & de Pablo (81). Belardinelli et al. (84) analyzed in more detail the time dependence of the error calculated with the $1/t$ algorithm and found that it varies as $N^{-1/2}$, where N is the number of Monte Carlo steps, in quantitative agreement with the simple sampling Monte Carlo method. More recently,

Zhou & Su (85) have also proposed a "1/t" rule and have shown that the convergence of the simulation is at least as good as with the conventional Monte Carlo algorithm, i.e., the statistical error vanishes as $1/t$, where t is the normalized time of the simulation. Importantly, they also prove that the error cannot vanish faster than $1/t$.

3. ADVANCED DENSITY OF STATES–BASED MONTE CARLO METHODS

As alluded to earlier, several ideas have been proposed to address the convergence of DOS-based Monte Carlo techniques. In the following we briefly highlight several such methods of particular importance for the study of complex systems.

3.1. Configurational Biased Density of States

The original WL DOS method was implemented on a 2D Ising model employing simple local moves (25). The free energy surface of molecular systems, such as proteins or polymers, is more complex, and more elaborate Monte Carlo trial moves are often required for efficient sampling. Jain & de Pablo (59) proposed a modified version of the traditional WL DOS that takes into account the use of advanced bias moves, in particular simple configurational bias (86, 87) and topological configurational bias (88) moves. The modified algorithm is similar to the traditional WL DOS, but the acceptance criteria must be adjusted. As described in the Supplemental Text, in deriving Equation E3 we assumed $P_{\text{propose}}(o \to n) = P_{\text{propose}}(n \to o)$. If a configurational bias is introduced, Equation E3 of the Supplemental Text must be rewritten as

$$\frac{P_{\text{accept}}(o \to n)}{P_{\text{accept}}(n \to o)} = \frac{\Omega(E_o) P_{\text{propose}}(n \to o)}{\Omega(E_n) P_{\text{propose}}(o \to n)}. \qquad 11.$$

Hence, the Metropolis acceptance criteria used in the case of a configurational bias DOS simulation becomes:

$$P_{\text{accept}}(o \to n) = \min\left[1, \frac{\Omega(E_o) P_{\text{propose}}(n \to o)}{\Omega(E_n) P_{\text{propose}}(o \to n)}\right]. \qquad 12.$$

The particular form of the function $P_{\text{propose}}(o \to n)$ depends on the details of the trial move (59).

3.2. Configurational Temperature Density of States

In traditional DOS simulations, the convergence factor f is decreased monotonically as the simulation proceeds. Configurations generated at different stages of the simulation therefore do not contribute equally to the running estimate of the free energy profile. As Yan & de Pablo (81) originally pointed out, in late stages of the simulation, the convergence factor is so small that the contribution of the corresponding configurations to the free energy becomes negligible. In other words, many of the configurations generated in a conventional WL DOS simulation are not utilized effectively, and increasing the simulation time does little to improve the final result of a simulation.

To circumvent this problem, Yan & de Pablo (81) realized that rather than updating directly the DOS through a random walk in energy space, one can actually update the derivative of the DOS with respect to energy and then integrate that function to arrive at $\Omega(E)$ (89). That derivative is the temperature,

$$\frac{1}{T} = \left(\frac{\partial S}{\partial E}\right)_V = k_B \left[\frac{\partial \ln \Omega(N, V, E)}{\partial E}\right]_V, \qquad 13.$$

which can be integrated to give the DOS according to

$$\ln \Omega(N, V, E) = \int_{E_0}^{E} \frac{1}{k_B T} \mathrm{d}E. \qquad 14.$$

Equation 14 requires that the temperature be known as a function of the energy. Yan & de Pablo (81) used the instantaneous configurational temperature (89), which can be determined from the particles' coordinates according to

$$\frac{1}{k_B T_{\text{config}}} = \frac{\left\langle -\sum_i \Delta_i \cdot F_i \right\rangle}{\left\langle \sum_i |F_i|^2 \right\rangle}, \qquad 15.$$

where F_i is the force acting on particle i. In their proposed random walk algorithm, which they referred to as configurational temperature DOS (CT DOS), the dynamically modified DOS serves only to guide the random walker through configuration space. The final thermodynamic DOS is calculated from the configurational temperature accumulated in the simulation according to Equation 14. Because all configurations generated throughout the simulation contribute equally to the estimated configurational temperature, the algorithm eliminates the problem of nonuniform contributions to the DOS encountered in traditional WL DOS sampling.

For systems in which the configurational temperature is not directly accessible (e.g., hard-sphere or lattice systems), Yan & de Pablo (81) also introduced a microcanonical formulation in which the sum of kinetic and potential energy is constant but the potential energy is allowed to fluctuate. The kinetic energy can then be used to estimate an instantaneous temperature, which is used as outlined above to calculate the DOS. In such an ensemble, the probability of observing a configuration $\mathbf{x}$ having total energy E and potential energy $U(\mathbf{x})$ is given by:

$$\pi(E, \mathbf{x}) \propto \frac{[E - U(\mathbf{x})]^{(l-2)/2} \Theta[E - U(\mathbf{x})]}{\Omega(N, V, E)}, \qquad 16.$$

where l is the total number of degrees of freedom of the system, Θ is the unit step function, and $\Omega(N, V, E)$ is the DOS corresponding to the total energy E, which is calculated on the fly as in a WL DOS simulation.

Figure 3 compares the performance of various algorithms for a truncated and shifted Lennard-Jones fluid. Results are shown for the statistical error as a function of convergence factor. For a given amount of computer time, the errors of the CT DOS method are much lower than those of a WL DOS simulation. Yan & de Pablo (81) estimate that for simple Lennard-Jones fluid simulations, their proposed approach is approximately two orders of magnitude faster than traditional WL DOS simulations. The CT DOS method is particularly effective for complex systems including proteins (62) and glasses (90).

3.3. Use of Multiple Windows

Dayal et al. (91) showed that the computational time required by DOS techniques scales as the exponential of the system size and the corresponding energy range. One way to circumvent this problem is to divide the energy range of interest into smaller ranges and then to combine the results from smaller simulations to generate the entire DOS for a broad energy domain. More specifically, Yan & de Pablo (81) divide a wide energy range into smaller, slightly overlapping energy windows. Independent WL DOS or CT DOS simulations are run in each of these energy windows, and configuration exchanges, or swap moves, are proposed between adjacent windows every N_{swap} steps. Once converged, the DOS functions corresponding to all windows are merged

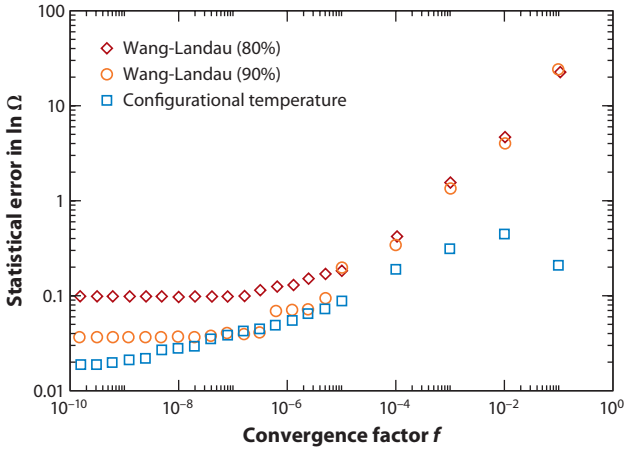

Figure 3

Performance of the configurational temperature density-of-states (CT DOS) algorithm as compared with normal Wang-Landau (WL) DOS simulations for a truncated and shifted Lennard-Jones liquid ($0.85 < T^* < 1.5$; $\rho^* = 0.78$). The percentage given in the label represents the degree of flatness of the histogram. For WL simulations, the errors reach an asymptotic value as the simulation time increases (or $\ln f$ decreases). For CT DOS simulations, the error decreases as simulation time increases. For a given amount of simulation time, the errors of CT DOS are smaller than those of WL DOS. Figure adapted from Reference 81.

to generate the DOS over the entire energy range of interest. Such an approach gives rise to the problem choosing the width of the windows, for which several strategies (92–95) are available.

Various attempts have been made to improve various aspects of multiple-window DOS simulations. Janosi & Doxastakis (96) proposed a particularly effective multiple-walker multiple-window approach. They divide the order parameter of interest into multiple overlapping windows. Each window is sampled by using multiple independent walkers (multiple realizations of the box). At regular intervals randomly chosen walkers from adjacent windows are swapped. The advantage of their method over traditional WL DOS simulations is evident in the results shown in **Figure 4** for a $Q = 10$ Potts model. The number of steps by a walker necessary to produce a flat histogram of energies in the late stages (small $\ln f$) of a DOS simulation is smaller when eight walkers are used than when a single walker is used (which corresponds to a WL simulation). This scheme is particularly helpful for implementation on parallel architectures. Janosi & Doxastakis (96) also demonstrated the advantages of using such an approach in conjunction with smart Monte Carlo moves.

3.4. Round-Trip Algorithms

An important concept in DOS-based simulations is the so-called tunneling time required for the random walker to travel from the lower bound of a given energy range to its upper bound. Ideally, that tunneling time should be as short as possible. Dayal et al. (91), however, have shown that for a 2D Ising model the tunneling time in a conventional flat-histogram WL DOS method increases significantly with system size N, thereby placing restrictions on the types of problems that WL DOS sampling simulations can address. Multiple windows can alleviate these restrictions, as mentioned earlier. They can also be circumvented by relaxing the flat-histogram condition of the original WL algorithm. Trebst et al. (97) have proposed an algorithm that systematically optimizes

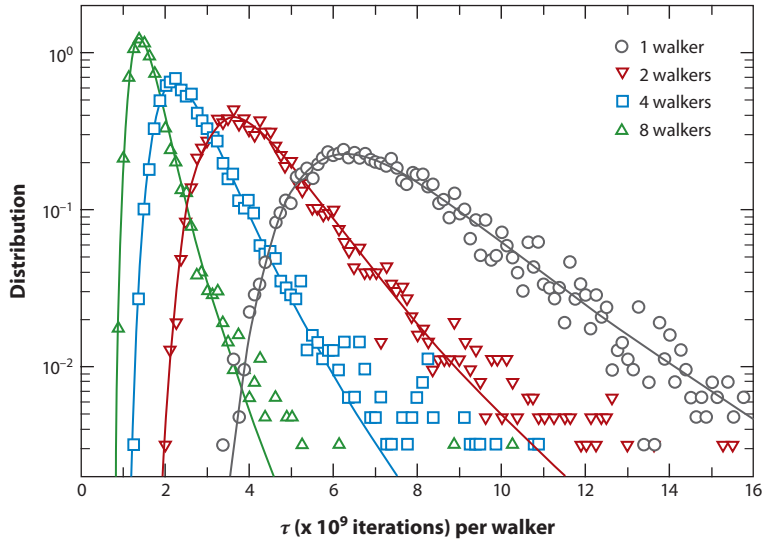

Figure 4

Advantages of the multiple-window multiple-walker algorithm over Wang-Landau density of states (DOS) simulations for a $Q = 10$ Potts model using different numbers of walkers. τ denotes the number of steps by a walker necessary to produce a flat histogram of energies in the late stages (small ln f) of a DOS simulation. The figure shows the normalized distribution of τ extracted from 5,000 independent simulations. Figure reprinted with permission from Reference 96. Copyright © 2009, American Institute of Physics.

the sampling in DOS-based simulations by maximizing the number of round trips between the low and the high end of the energy range. Such an approach implicitly leads to minimization of the tunneling time. To measure the number of round trips, these authors defined two types of walkers: unlabeled and labeled (+ and –, respectively, with distributions given by n_+ and n_-). The labels indicate which of the two extrema of the energy space the walker last visited. The two extrema of the energy window act as reflecting and absorbing boundaries for the labeled walkers: if the label is +, a visit to the upper energy bound does not change the label, whereas a visit to the lower energy bound leads the walker to change its label from + to −. The fraction of time that a walker is labeled + is given by $f(E) = \frac{n_+(E)}{n_w(E)}$, where $n_w(E)$ denotes the number of times the system has visited an energy value of E when w weights are applied to it. A current j can then be defined to quantify the flow of labeled walkers according to

$$j = D(E)n_w(E)\frac{\mathrm{d}f}{\mathrm{d}E}, \qquad 17.$$

where $D(E)$ represents the labeled walker's diffusivity. Noting that at steady state the current j should be constant and that $f(E)$ satisfies the boundary conditions $f(E_{\max}) = 1$ and $f(E_{\min}) = 0$, Equation 17 can be written as:

$$\frac{1}{j} = \int_{E_{\min}}^{E_{\max}} \frac{\mathrm{d}E}{D(E)n_w(E)}. \qquad 18.$$

To maximize the number of round trips in a given energy range, Equation 18 needs to be minimized under the constraint that $n_w(E)$ is a probability distribution function. Using an Euler-Lagrange relation, the optimal solution is

$$n_w^{\text{optimal}} = \frac{1}{D(E)\lambda}, \qquad 19.$$

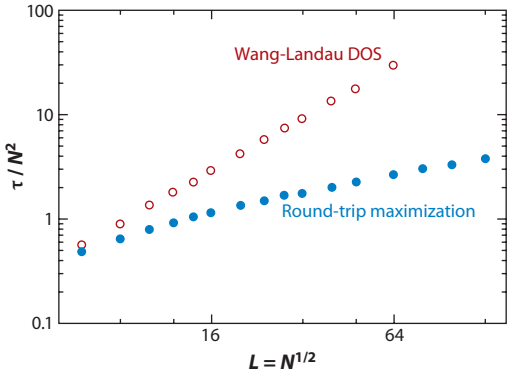

Figure 5

Scaling of round-trip times (τ) in the energy interval [$-N$,0] for the 2D fully frustrated Ising model with N spins using Metropolis dynamics. The open red symbols show results from Wang-Landau density of states (DOS) simulations, and the filled blue symbols show results from the round-trip maximization algorithm. The points correspond to results presented in Reference 97.

where λ is an arbitrary constant. The problem is therefore one of finding the diffusivity $D(E)$ of labeled walkers. Trebst et al. (97) proposed an iterative feedback algorithm to estimate $D(E)$ in which simulations begin with arbitrary weights $w(E)$. A fixed number of Monte Carlo steps are performed, and the weights are modified according to the collected statistics using a set of rules that are based on Equation 19:

$$\ln w(E)^{(\text{new})} = \ln w(E)^{(\text{old})} + 0.5\left[\ln \frac{\mathrm{d}f}{\mathrm{d}E} - \ln n_w(E)^{(\text{old})}\right]. \qquad 20.$$

The feedback loop continues until the weights stop changing.

Trebst et al. (97) showed that, using this algorithm, the relative statistical error in the DOS scales as $\mathcal{O}(1/N^{1/2}_{\text{round trips}})$. For the 2D ferromagnetic and fully frustrated Ising models, round-trip times, τ, from the ground state to the maximum entropy state scale as $\mathcal{O}[(N \ln N)^2]$, which represents a significant increase compared with the power-law behavior $\mathcal{O}(N^{2+z})$ of conventional flat-histogram DOS algorithms, where $0 < z \leq 1$. Results for the Ising model system are given in **Figure 5**; for simple systems, the advantage of flux methods over flat-histogram approaches is evident. Note, however, that in order for the round-trip approach to be effective for systems having low diffusivity along reaction coordinates (such as proteins), one must provide a good initial guess of the density of states. Escobedo & Martínez-Veracoechea (98, 99) have presented an extension of Trebst et al.'s (97) work for EXEDOS simulations.

3.5. Use of Rejected States to Enhance Sampling

All of the DOS-based methods described above rely on the original Metropolis concept (77) in which only accepted trial moves are used to compute thermodynamic averages. Rejected states are never used to estimate observables such as the DOS. Frenkel (100) showed that rejected states can in fact be used in traditional Monte Carlo simulations to improve sampling. Chopra & de Pablo (101) subsequently showed that rejected states can also be included in WL DOS and CT DOS algorithms to improve sampling and the overall performance of DOS-based simulations.

To include rejected states in the WL DOS algorithm, a single WL DOS step between two states, o to n, is replaced by M WL DOS steps, where M is a large number. The states o and n

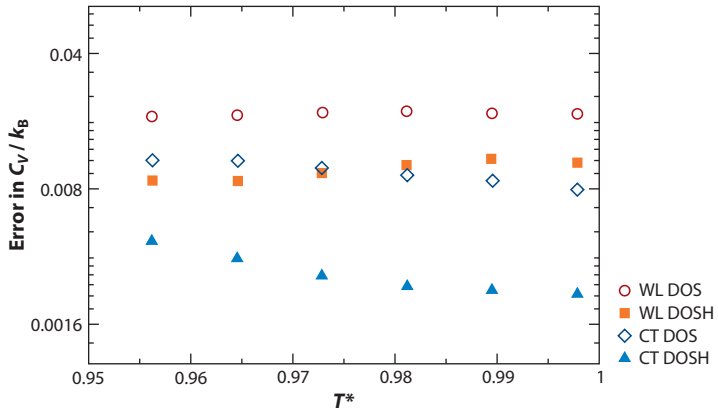

Figure 6

Statistical errors in the calculation of specific heat (C_V / k_B) for a truncated and shifted Lennard-Jones liquid ($\rho^* = 1$). For a given amount of computer time, the configurational temperature density of states (CT DOS) method with the use of rejected states (CT DOSH) provides results of greater accuracy than those obtained by a traditional Wang-Landau (WL) DOS method. Figure adapted with permission from Reference 101. Copyright © 2006, American Institute of Physics.

will be referred to as microstates and the M intermediate WL DOS steps as microsteps. These microsteps are analogous to the sampling of a Markovian web in Reference 100. If out of M microsteps, M_o steps are taken to state o (and M_n steps to state n), and if in every visit to o (or n) the DOS Ω is updated according to $\Omega(E_o) = \Omega(E_o) f$ [or $\Omega(E_n) = \Omega(E_n) f$], where f is an arbitrary modification factor, then, in effect, after M microsteps, $\Omega(E_o)$ is modified to $\Omega(E_o) f^{M_o}$ [and $\Omega(E_n)$ to $\Omega(E_n) f^{M_n}$]. In the limit of M going to infinity, M_o (or M_n) is given by $M_o = M\mathcal{P}(o)$ [and $M_n = M\mathcal{P}(n)$], where $\mathcal{P}(s)$ is the probability of visiting state s during the microsteps. The probability $\mathcal{P}(s)$ in DOS simulations is proportional to $1/\Omega(E_s)$; for the microsteps, $\mathcal{P}(o)$ is given by $\Omega(n)/(\Omega(o) + \Omega(n))$, and $\mathcal{P}(n)$ is given by $\Omega(o)/[\Omega(o) + \Omega(n)]$. After the microsteps, the DOS Ω is updated according to:

$$\Omega(E) = \begin{cases} \Omega(E_o) f^{\frac{\Omega(n)}{[\Omega(o)+\Omega(n)]}}, & \text{if} \quad E = E_o \\ \Omega(E_n) f^{\frac{\Omega(o)}{[\Omega(o)+\Omega(n)]}}, & \text{if} \quad E = E_n \\ \Omega(E), & \text{if} \quad E \neq E_0 \text{ or } E_n. \end{cases} \qquad 21.$$

No histogram update is performed during the microsteps. The remainder of the algorithm is identical to that of a conventional DOS simulation. The analysis for the CT DOS algorithm is similar. As illustrated in **Figure 6**, Chopra & de Pablo (101) reported that for DOS simulations of a simple Lennard-Jones liquid, CT DOS with the use of rejected states provides results that are more accurate than those obtained by a traditional WL DOS method for a comparable amount of simulation time.

3.6. Additional Improvements to Density of States Simulations

Additional improvements to the original WL DOS approach rely on the concept of parallel tempering (20, 21) or replica exchange (22). Fenwick & Escobedo (61), for example, have shown that EXEDOS simulations can be improved by applying a small number of replicas. Another improvement to DOS approaches, suggested by Shell et al. (102), seeks to accelerate the time required to

reach a flat histogram by providing an estimate of the initial DOS guess that relies on infinite-temperature transition probabilities, i.e., the probabilities associated with a move proposal only.

4. ADVANCES IN METADYNAMICS

As was the case for traditional DOS simulations, some of the central concerns in metadynamics simulations are related to convergence. The issue of convergence in metadynamics is perhaps more severe because, as originally proposed, the method relies on a continuous influx of energy into the system throughout the entire duration of a molecular dynamics simulation; detailed balance is not satisfied asymptotically, as was the case in Monte Carlo DOS-based approaches. Several strategies (74–76, 103–107) have been proposed in recent years to address such concerns. Most of these represent ad-hoc solutions; mathematical proofs of convergence have been scarce. We discuss several of these techniques below, and, for a few simple model systems, we provide comparative results.

Metadynamics yields a free energy profile $F(s)$ as a function of an order parameter s. One of the simplest methods to deal with the problem of convergence involves a simple averaging of $F(s)$ performed over the final portion of a regular metadynamics simulation run. Mathematically, the converged free energy curve is given by:

$$F(s) = \frac{1}{\tau}\int_{\mathcal{T}-\tau}^{\mathcal{T}} \mathrm{d}t F(s,t), \qquad 22.$$

where τ represents the time over which the averaging is performed and $\mathcal{T}$ represents the total time for a metadynamics run. It has been shown numerically that such an approach works for a model Langevin system without memory friction or inertia (108) and for a 2D Ising model (109) using Monte Carlo metadynamics. For more complex systems in which the free energy is unknown a priori, it is unclear whether this approach would work and how parameters τ and $\mathcal{T}$ would influence the results.

4.1. Flat-Histogram Metadynamics

Min et al. (76) have proposed another solution to the problem of convergence in metadynamics based on flat-histogram ideas from WL DOS simulations. They start a regular metadynamics simulation with large hill heights and collect a histogram of visits to distinct order parameter states. Once that histogram is sufficiently flat, the hill heights are decreased. In a sense, the hill heights being added plays a role analogous to that of the modification factor f in DOS-based algorithms. As the hill heights become smaller, the condition of detailed balance is satisfied asymptotically, similar to the case of WL DOS simulations. After several metadynamics cycles, the hills are so small that the free energy surface $F(s)$ changes only negligibly, thereby leading to a converged free energy surface. Mathematically, the distribution of the system, i.e., the histogram $n_w(s)$, is given by $n_w(s) \propto w(s)\Omega(s)$, where $w(s)$ represents the bias applied to the system to ensure uniform sampling of the order parameter space and $\Omega(s)$ is the DOS of the system. In this notation, $n_w(s)$ denotes the number of times that a state s is visited for a given applied weight $w(s)$. In the spirit of DOS approaches, once the histogram is flat and $n_w(s)$ is constant, the free energy $F(s)$ is given by:

$$\frac{F(s)}{k_B T} = \ln w(s) = -\ln \Omega(s). \qquad 23.$$

As noted before, in traditional metadynamics, the free energy surface $F(s)$ is given by the negative of the added Gaussian potentials $-V_G(s)$. Hence, we see from Equation 23 that the added

Gaussian potentials are analogous to the weights applied to ensure uniform sampling: $\ln w(s) = -\ln \Omega(s) = -\frac{V_G(s)}{k_B T}$. More generally, in metadynamics, the additional Gaussian potential terms can be seen as the set of weights $w(s)$ applied to the system to ensure uniform sampling of the complete order parameter space. Such a result provides a direct link between DOS-based methods and the metadynamics approaches that rely on molecular dynamics simulations to evolve the system.

4.2. Well-Tempered Metadynamics

Barducci et al. (110) have proposed an alternative means to improve convergence, the so-called well-tempered metadynamics (WTM) method, which is inspired by ideas from the self-healing umbrella sampling technique (72). In WTM, the order parameter space s is sampled at an elevated temperature $T + \Delta T$. For a system with a single collective variable s, the sum of added Gaussian potentials at any time t is given by

$$V_G(s,t) = W \sum_{t' \le t} \exp\left[-\frac{V_G(s,t')}{\Delta T}\right] \exp\left\{-\frac{[s - s(t')]^2}{2\delta s^2}\right\}, \quad 24.$$

where all parameters have the same meaning as in Equation 10. Parameter ΔT controls the rate of decay for the height of the added Gaussian potentials or hills. The final free energy is given by

$$F(s) = -\frac{T + \Delta T}{\Delta T} V_G(s,t). \quad 25.$$

When $\Delta T \to \infty$, WTM approaches the traditional metadynamics technique, and when $\Delta T \to 0$, it approaches an unbiased simulation. It has been shown mathematically that, in the long time limit, WTM leads to a converged free energy surface. The time for convergence, however, depends strongly on the values of parameters W, δs, and ΔT. Given that the actual free energy profile is not known a priori, for complex systems it can be challenging to identify an optimal set of parameters that leads to efficient convergence of the algorithm.

4.3. Flux-Tempered Metadynamics

As mentioned earlier, metadynamics can be linked directly to DOS-based approaches. Dayal et al.'s (91) concerns about the limitations of flat-histogram-based sampling algorithms therefore extend to metadynamics. Recently, Singh et al. proposed an algorithm, known as flux-tempered metadynamics (FTM) (107), that addresses convergence using ideas from round-trip maximization (see Section 4.4). Based on the equivalence between $\ln w(s)$ and the added Gaussian potentials $V_G(s)$, as described with respect to the flat-histogram method proposed by Min et al. (76), Equation 20 can be rewritten for metadynamics as:

$$\begin{aligned} &V_G(s)^{(\text{new})} = V_G(s)^{(\text{old})} + m(s), \\ &\text{where } m(s) = -\frac{1}{2} k_B T \left[\ln \frac{df}{ds} - \ln n_w(s)^{(old)}\right]. \end{aligned} \quad 26.$$

Similar to the strategy of Trebst et al. (97), the FTM method is iterative in nature, and detailed balance is satisfied. One major advantage of FTM over other versions of metadynamics is that the simulated free energy surface does not depend on the actual metadynamics parameters such as the hill height W or hill width δs.

It is instructive to compare the performance of various versions of metadynamics on a simple toy model. In what follows we consider an isolated butane-like molecule in a vacuum. For details on the system, readers are referred to Reference 107. Four variants of metadynamics are considered

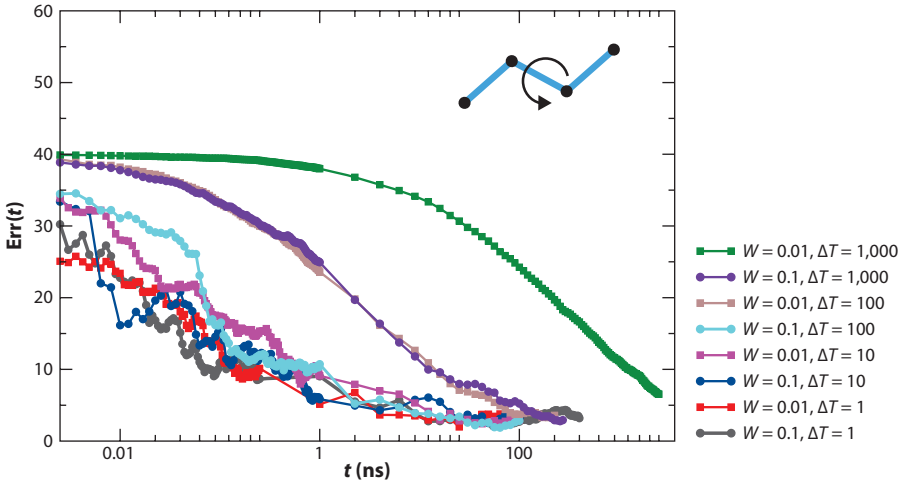

Figure 7

Error as a function of simulation time (see Equation 27) in the free energy of an isolated butane-like molecule as a function of the dihedral angle when different values of the hill height W and parameter ΔT are used for well-tempered metadynamics simulations.

here. In all cases, hills were added every 0.1 ps. First, a conventional metadynamics algorithm was implemented using two values of hill height W, namely 0.1 kcal mol^{-1} and 0.01 kcal mol^{-1}. Second, for the WTM method, all simulations were performed with an initial hill height of 0.1 kcal mol^{-1}. The optimal value of the parameter ΔT in Equation 24 was determined by trial and error. Determination of an optimal value of this parameter is possible only because of the simplicity of the butane-like molecule; for more complex systems, such determination can be challenging. **Figure 7** shows the effect of different parameters on the quality of the simulated free energy as a function of dihedral angle. One can see that a poor choice of parameters can lead to convergence times that differ by more than three orders of magnitude.

Third, the flat-histogram metadynamics proposed by Min et al. (76) was implemented with an initial hill height of 0.1 kcal mol^{-1}. Finally, FTM was implemented as outlined in Reference 107. The initial guess for the FTM method was generated from a conventional metadynamics run for 500 ps with a hill height of 0.01 kcal mol^{-1}. The resulting free energy profiles for all four methods after a simulation run of 1 ns are plotted in **Figure 8**.

The FTM method is able to generate a converged free energy profile relatively quickly, whereas the other metadynamics variants yield free energy profiles that exhibit considerably larger errors. The convergence can be quantified through the following definition of the error in $F(s)$:

$$\mathrm{Err}(t) = \inf_{C \in \mathbb{R}} \int_{s_-}^{s_+} \mathrm{d}s \, \left| F(s,t) - F_{\mathrm{analytical}}(s) - C(t) \right|, \qquad 27.$$

where $F(s,t)$ is the free energy obtained from any method at time t, $F_{\mathrm{analytical}}(s)$ is the analytical (exact) free energy curve, and the optimal value of $C(t)$ is found using a least-squares fit. **Figure 9** shows the error function as defined in Equation 27 for the butane-like molecule. The FTM method proposed here converges in 1 ns, faster than all other methods (which require more than 5 ns to converge). More importantly, the error Err(t) in the free energy profile generated by the FTM method is considerably smaller [Err(t) $\approx$ 0.6] than that obtained with other methods [Err(t) $\geq$ 3.3].

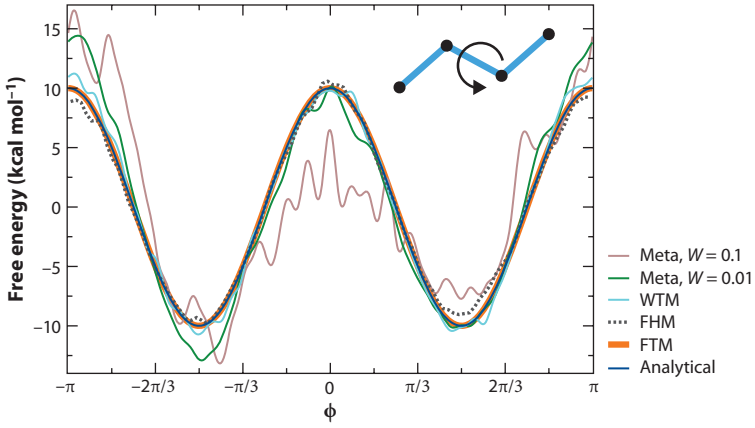

Figure 8

Free energy as a function of dihedral angle as obtained by several methods after a simulation run of 1 ns for an isolated butane-like molecule. Abbreviations: FHM, flat-histogram metadynamics; FTM, flux-tempered metadynamics; Meta, metadynamics; WTM, well-tempered metadynamics. Figure adapted from Reference 107.

The FTM simulations can be particularly helpful for more complex systems, including proteins. **Figure 10** shows results for the extension of a 15-residue helical polyalanine peptide in explicit water from different types of metadynamics simulations and from an extensive umbrella sampling simulation; statistics were collected over 2 μs of simulation time. To generate an acceptable free energy profile [error function (from Equation 27) $\leq$ 1], the FTM converges several orders of magnitude faster than the other metadynamics methods considered here.

Several other approaches (106, 111, 112) that have been proposed to address the issue of convergence avoid calculating a free energy profile directly from metadynamics. Babin et al. (106)

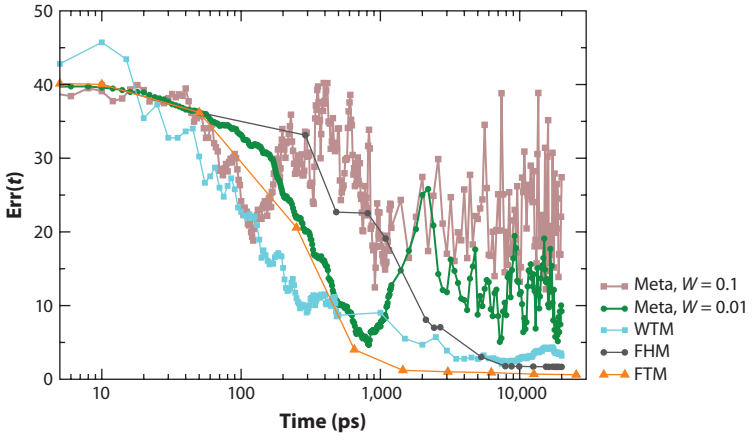

Figure 9

Error as a function of simulation time (see Equation 27) in free energy profile as a function of time for different simulation methods for an isolated butane-like molecule. Abbreviations: FHM, flat-histogram metadynamics; FTM, flux-tempered metadynamics; Meta, metadynamics; WTM, well-tempered metadynamics. Figure adapted from Reference 107.

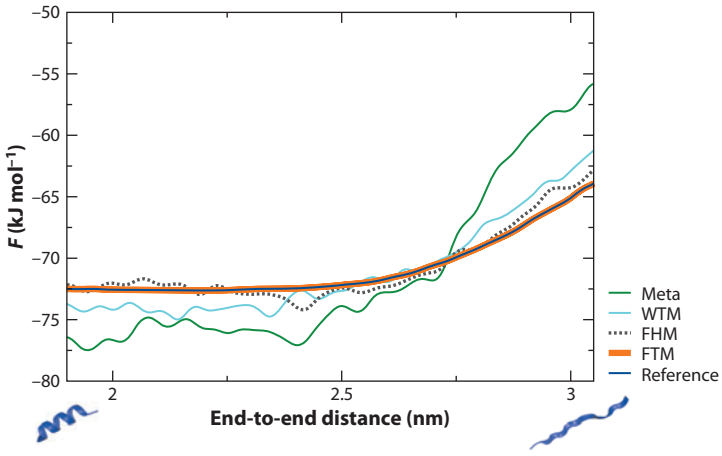

Figure 10

Free energy as a function of end-to-end distance as obtained by several methods after a simulation run of 20 ns for extension of a 15-residue polyalanine peptide (structures shown below graph) in explicit water (solvent not shown for clarity). The reference free energy is from an umbrella sampling simulation with 40 windows in the order parameter range of interest (1.7–3.1 nm) and 50 ns of simulation time for each window. Abbreviations: FHM, flat-histogram metadynamics; FTM, flux-tempered metadynamics; Meta, metadynamics; WTM, well-tempered metadynamics.

and Zhang & Voth (112), for example, use metadynamics to identify a minimum free energy path and then use this information to perform umbrella sampling (47) simulations to arrive at a final converged free energy profile. Li et al. (111) perform metadynamics in energy space. Once a rough bias is obtained, a new simulation is started with a fixed bias. The final free energy is obtained from the statistics generated from the fixed bias simulations and by applying a weighted histogram analysis (113, 114) with the applied bias.

Beyond the issue of convergence, several authors have examined the accuracy, speed, and parameter dependence of metadynamics. For conventional metadynamics, Laio et al. (115) have quantified the dependence of the resulting errors on different metadynamics parameters for a model Langevin system without memory friction or inertia according to:

$$\bar{\epsilon} = C(d)\sqrt{\frac{S\delta s}{D\tau_G}\frac{W}{\beta}}, \qquad 28.$$

where $C(d)$ represents the lower bound to the error, S is the system size, D is the diffusivity of the system in the collective variable space, β is the inverse temperature, W is the height of the added hills, τ_G is the frequency of hill addition, and δs is the width of the hills. Laio et al. (115) conclude that the easier it is for the variable s to diffuse through the region of interest (equivalent to a large value of D), the better the accuracy will be. The error in general increases as the region explored by metadynamics, S, becomes bigger or topologically more complex, which suggests that the method should be used with caution for reconstructing the free energy profile on large regions or on free energy surfaces containing many basins connected by narrow paths.

The application of metadynamics for simulation of complex systems is limited by the choice of collective variables. Ideally, one should use the slowest reaction coordinates to fill the hills; in practice, such coordinates are seldom known. In the absence of well-defined strategies for selection of optimal collective variables, it is common to work simultaneously with multiple collective

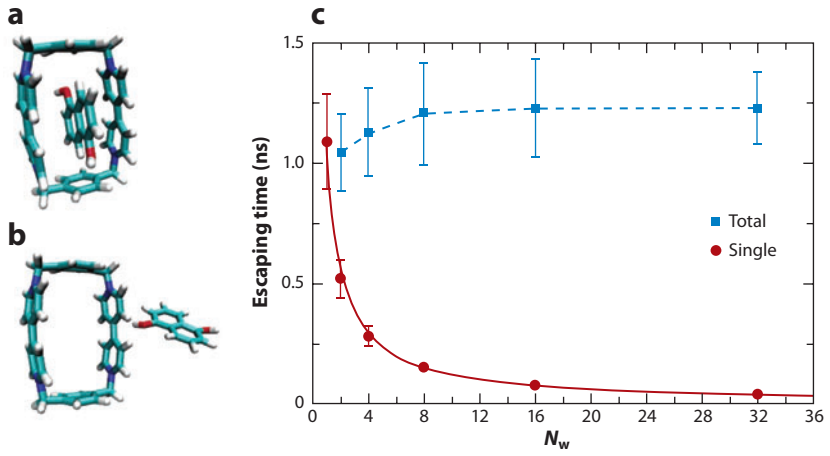

Figure 11

(*a*) A cyclophane ring and (*b*) 1,5-dihydroxynaphthalene are solvated in acetonitrile (solvent not shown for clarity). (*c*) Total simulation time (*blue squares*) and time simulated by each walker (*red circles*) required for one walker to escape from the starting well, averaged over 10 independent simulations, as a function of the number of walkers (N_w). The total time is almost constant, whereas the time required per walker decreases as $1/N_w$, which indicates that the algorithm scales linearly. Figure adapted with permission from Reference 116. Copyright © 2006 American Chemical Society.

variables. The obvious problem with such an approach is one of computational resources: the time required for a traditional metadynamics simulation follows a power-law dependence on the number of collective variables. The next section describes several improvements to enhance sampling with a suboptimal choice of collective variables.

4.4. Multiple Walkers in Metadynamics

With the advent of multicore computers, multiple simulations of the same system can be run in parallel. In Raiteri et al.'s (116) approach, multiple walkers are used to explore the same free energy surface. Each walker contributes to a history-dependent potential that, in metadynamics, serves as an estimate of the free energy. In particular, the free energy surface from a multiple-walker simulation with N_w walkers is given by:

$$F_G(\mathbf{s}, t) = \frac{W}{\tau_G} \sum_{i=1}^{N_w} \int_0^t dt' \exp\left(-\frac{|\mathbf{s} - \mathbf{s}_i(t')|^2}{2|\delta s|^2}\right), \quad 29.$$

where $\mathbf{s}_i$ is the position of the i^{th} walker and other symbols have the same meaning as in Equation 10.

The idea presented in this method can be connected to the results of Equation 28. As the error in the free energy is inversely proportional to the diffusivity of the walkers, by increasing that quantity the error in the free energy surface can be decreased significantly. Representative results for a real complex of a tetracationic cyclophane and a 1,5-dihydroxynaphthalene solvated in acetonitrile are shown in **Figure 11** (116). This system is known to have two energy minima states separated by an energy barrier of ≈15 kJ mol^{-1}. Raiteri et al. (116) showed that the error in the calculated free energy surface is independent of the number of walkers. They also showed that the maximum number of allowed walkers grows exponentially with the dimensionality of the free energy that is desired. For more complex systems, larger numbers of walkers can be used.

4.5. Parallel Tempered Metadynamics

Parallel tempering or replica exchange (20, 21, 22, 35, 117, 118) is commonly used to improve sampling in Monte Carlo and molecular dynamics simulations. Bussi et al.'s (119) method combines the ideas of parallel tempering with metadynamics. Consistent with conventional implementations of parallel tempering (20, 21, 22, 35, 118), multiple replicas of the system are run simultaneously at different temperatures. Although a conventional metadynamics (73) simulation is carried out on each replica independently, configurations between neighboring replicas are exchanged periodically subject to a Metropolis acceptance criterion. The acceptance ratio for an exchange involving replicas i and j is given by:

$$p_{ij}^{\text{accept}} = \min\Big[1, \exp\Big((\beta_j - \beta_i)[U(\boldsymbol{x}_j) - U(\boldsymbol{x}_i)] + \beta_i\Big\{V_G^i[s(\boldsymbol{x}_i)] - V_G^i[s(\boldsymbol{x}_j)]\Big\} + \beta_j\Big\{V_G^j[s(\boldsymbol{x}_j)] - V_G^j[s(\boldsymbol{x}_i)]\Big\}\Big)\Big], \quad 30.$$

where U is the potential energy of a system and $\mathbf{x}$ represents the coordinates of the system. If an exchange is accepted, the coordinates are exchanged and momenta $\boldsymbol{p}$ are rescaled according to

$$\boldsymbol{x}_i' = \boldsymbol{x}_j; \quad \boldsymbol{p}_i' = \sqrt{\frac{\beta_j}{\beta_i}}\,\boldsymbol{p}_j, \quad 31.$$

$$\boldsymbol{x}_j' = \boldsymbol{x}_i; \quad \boldsymbol{p}_j' = \sqrt{\frac{\beta_j}{\beta_i}}\,\boldsymbol{p}_i. \quad 32.$$

As the simulation proceeds, the biases corresponding to different temperatures tend to compensate for the corresponding free energies, and the various CVs start diffusing freely on a barrier-less landscape. This leads to a significant decrease in the autocorrelation time.

4.6. Bias-Exchange Metadynamics

A common feature of most parallel tempering simulations is that many replicas are required for correct and optimal sampling. An exception is provided by Faller et al. (117), who introduced parallel tempering in a multicanonical ensemble. In this approach, multicanonical weights are derived by a self-consistent iterative process using a Boltzmann inversion of global energy histograms. Such a procedure gives rise to a much broader overlap of thermodynamic-property histograms, thereby reducing the number of replicas necessary to cover an energy range. Similarly, for complex and large systems, many temperature replicas are generally required to sample the slowest CVs. Along the same vein, Piana & Laio (120) have proposed a modification of metadynamics in which multiple replicas are simulated in different boxes at the same temperature but with different biases. This approach is particularly helpful for systems in which a reasonable set of slow CVs can be guessed a priori. In this way, only a few replicas are necessary. In addition to running replicas in which a bias is applied, an additional replica with no bias is also simulated. The replicas with biasing help enhance sampling, but the final free energy is calculated on the basis of statistics generated in the replica with no bias. The acceptance criteria for trial exchanges between replicas i and j are given by

$$p_{ij}^{\text{accept}} = \min\Big(1, \exp\Big\{\beta\Big[V_{\text{G}}^i(\boldsymbol{x}_i, t) + V_{\text{G}}^j(\boldsymbol{x}_j, t) - V_{\text{G}}^i(\boldsymbol{x}_j, t) - V_{\text{G}}^j(\boldsymbol{x}_i, t)\Big]\Big\}\Big). \quad 33.$$

If an exchange move is accepted, the collective variables jump from $s_i(\boldsymbol{x}_i)$ to $s_i(\boldsymbol{x}_j)$ and from $s_j(\boldsymbol{x}_j)$ to $s_j(\boldsymbol{x}_i)$. This method is helpful in simulations of the structure of unknown peptides. However, it does not yield the free energy profile of the system to within an arbitrary accuracy. The calculated free energy profile depends on the statistics generated from a given simulation run, and there are no criteria for stopping a calculation. The idea of running multiple replicas under different potentials has been used more generally (121) where biasing may not be guided by metadynamics. Recently, Smiatek & Heuer (122) proposed a method that applies the histogram reweighing technique described in Section 3.4 in the context of metadynamics simulations (see **Supplemental Text**). Such an approach can also be applied to bias-exchange simulations; in that case, one could in principle rely on statistics generated from all replicas to determine a free energy.

4.7. Self-Learning Metadynamics

Another recent development in the area of metadynamics aims to accelerate simulations by constructing a bias potential in terms of a patchwork of 1D, locally valid collective coordinates. For complex systems, typically several collective variables are important for effective sampling in metadynamics. Determination of such collective variables is challenging. In self-learning metadynamics (123), such collective coordinates adapt to any new features encountered during the simulation. The performance of self-learning metadynamics has been discussed recently in the context of model proteins with promising results (123). However, as in traditional metadynamics, the self-learning method does not guarantee convergence.

5. CONCLUDING REMARKS

The central aim of this review is to provide a general overview of novel simulation algorithms proposed within the past decade, in which the sampling or exploration of phase space is guided by the density of states or entropy of the system. In these algorithms, the DOS is not known a priori, but it evolves toward a converged value as the simulation proceeds, thereby providing the entropy or free energy of the system as one of the outcomes of the simulation. The methods discussed here have been organized into two classes, namely, Monte Carlo based and molecular dynamics based. The former build upon the original DOS algorithm proposed by Wang and Landau at the turn of the century, and the latter rely on the metadynamics ideas originally proposed by Laio and Parrinello. Monte Carlo approaches are powerful and flexible, but their application generally has been limited to relatively simple systems. In contrast, molecular dynamics–based methods are somewhat constrained in that they rely on modifications to Newton's equations of motion, but they are easily applicable to complex macromolecular systems, including biological molecules, in large part owing to the availability of public domain software [PLUMED is a software package (124) that implements metadynamics in several well-known simulation packages].

Two severe outstanding challenges include the issue of convergence and that of identifying appropriate order parameters or CVs to guide the sampling of phase space. To date, convergence has been examined more convincingly in the context of Monte Carlo–based DOS approaches. With regard to the choice of CVs or order parameters, a pressing issue is that of developing systematic approaches to identify suitable, slow variables upon which efficient sampling algorithms can be built.

Although this review is not exhaustive, one of our goals is to introduce new practitioners of molecular modeling to several of what we consider to be the more advanced and powerful simulation techniques proposed in recent years. For each approach, we have emphasized some of the shortcomings of existing techniques, and we have presented some of the emerging strategies,

however imperfect they may be, that experts have proposed to address such limitations. There is considerable room for refinement and for further advances, but as illustrated in this review, DOS-based methods have already provided enormous improvements over conventional simulation techniques for the study of complex molecular systems.

DISCLOSURE STATEMENT

The authors are not aware of any affiliations, memberships, funding, or financial holdings that might be perceived as affecting the objectivity of this review.

ACKNOWLEDGMENTS

The preparation of this review was supported by the Department of Energy, Basic Energy Sciences, Biomaterials Program, DE-SC0004025, and by the National Institutes of Health, grant NIH-1R01DK088184.

LITERATURE CITED

1. Landau DP, Binder K. 2000. *A Guide to Monte Carlo Simulations in Statistical Physics*. Berlin: Cambridge Univ. Press
2. Tuckerman ME. 2010. *Statistical Mechanics: Theory and Molecular Simulations*. New York: Oxford Univ. Press
3. Frenkel D, Smit B. 2001. *Understanding Molecular Simulations From Algorithms to Applications*. London: Academic
4. McQuarrie DA. 2000. *Statistical Mechanics*. Sausalito, CA: Univ. Sci. Books
5. Widom B. 1963. Some topics in the theory of fluids. *J. Chem. Phys.* 39:2808–12
6. Torrie GM, Valleau JP. 1977. Non-physical sampling distributions in Monte-Carlo free-energy estimation—umbrella sampling. *J. Comput. Phys.* 23:187–99
7. Beveridge DL, Dicapua FM. 1989. Free-energy via molecular simulation: applications to chemical and biomolecular systems. *Annu. Rev. Biophys. Biophys. Chem.* 18:431–92
8. Carter EA, Ciccotti G, Hynes JT, Kapral R. 1989. Constrained reaction coordinate dynamics for the simulation of rare events. *Chem. Phys. Lett.* 156:472–77
9. Straatsma TP, McCammon JA. 1991. Multiconfiguration thermodynamic integration. *J. Chem. Phys.* 95:1175–88
10. Berg BA, Neuhaus T. 1991. Multicanonical algorithms for first order phase transitions. *Phys. Lett. B* 267:249–53
11. Berg BA, Neuhaus T. 1992. Multicanonical ensemble: a new approach to simulate first-order phase transitions. *Phys. Rev. Lett.* 68:9–12
12. Lyubartsev AP, Martsinovski AA, Shevkunov SV, Vorontsov-Velyaminov PN. 1992. New approach to Monte Carlo calculation of the free energy: method of expanded ensembles. *J. Chem. Phys.* 96:1776–83
13. Kollman P. 1993. Free-energy calculations: applications to chemical and biochemical phenomena. *Chem. Rev.* 93:2395–417
14. Huber T, Torda AE, Vangunsteren WF. 1994. Local elevation: a method for improving the searching properties of molecular dynamics simulation. *J. Comput. Aided Mol. Des.* 8:695–708
15. Hansmann UHE, Okamoto Y. 1996. Monte Carlo simulations in generalized ensemble: multicanonical algorithm versus simulated tempering. *Phys. Rev. E* 54:5863–65
16. Escobedo FA, de Pablo JJ. 1996. Expanded grand canonical and Gibbs ensemble Monte Carlo simulation of polymers. *J. Chem. Phys.* 105:4391–94
17. Jarzynski C. 1997. Nonequilibrium equality for free energy differences. *Phys. Rev. Lett.* 78:2690–93
18. den Otter WK, Briels WJ. 1998. The calculation of free-energy differences by constrained molecular-dynamics simulations. *J. Chem. Phys.* 109:4139–46

19. Sprik M, Ciccotti G. 1998. Free energy from constrained molecular dynamics. *J. Chem. Phys.* 109:7737–44
20. Yan Q, de Pablo JJ. 1999. Hyper-parallel tempering Monte Carlo: application to the Lennard-Jones fluid and the restricted primitive model. *J. Chem. Phys.* 111:9509–16
21. Yan QL, de Pablo JJ. 2000. Hyperparallel tempering Monte Carlo simulation of polymeric systems. *J. Chem. Phys.* 113:1276–82
22. Sugita Y, Okamoto Y. 2000. Replica-exchange multicanonical algorithm and multicanonical replica-exchange method for simulating systems with rough energy landscape. *Chem. Phys. Lett.* 329:261–70
23. Hayryan S, Hu CK, Hu SY, Shang RJ. 2001. Multicanonical parallel simulations of proteins with continuous potentials. *J. Comput. Chem.* 22:1287–96
24. Darve E, Pohorille A. 2001. Calculating free energies using average force. *J. Chem. Phys.* 115:9169–83
25. Wang FG, Landau DP. 2001. Determining the density of states for classical statistical models: a random walk algorithm to produce a flat histogram. *Phys. Rev. E* 64:056101
26. Wang FG, Landau DP. 2001. Efficient, multiple-range random walk algorithm to calculate the density of states. *Phys. Rev. Lett.* 86:2050–53
27. Kim EB, Faller R, Yan Q, Abbott NL, de Pablo JJ. 2002. Potential of mean force between a spherical particle suspended in a nematic liquid crystal and a substrate. *J. Chem. Phys.* 117:7781–87
28. Calvo F. 2002. Sampling along reaction coordinates with the Wang-Landau method. *Mol. Phys.* 100:3421–27
29. de Pablo JJ, Escobedo FA. 2002. Molecular simulations in chemical engineering: present and future. *AIChE J.* 48:2716–21
30. Darve E, Wilson MA, Pohorille A. 2002. Calculating free energies using a scaled-force molecular dynamics algorithm. *Mol. Simul.* 28:113–44
31. Berg BA. 2003. Multicanonical simulations step by step. *Comput. Phys. Commun.* 153:397–406
32. Hove J. 2004. Density of states determined from Monte Carlo simulations. *Phys. Rev. E* 70:056707
33. Landau DP, Tsai SH, Exler M. 2004. A new approach to Monte Carlo simulations in statistical physics: Wang-Landau sampling. *Am. J. Phys.* 72:1294–302
34. Kofke DA. 2005. Free energy methods in molecular simulation. *Fluid Phase Equilib.* 228:41–48
35. Earl DJ, Deem MW. 2005. Parallel tempering: theory, applications, and new perspectives. *Phys. Chem. Chem. Phys.* 7:3910–16
36. Khan MO, Kennedy G, Chan DYC. 2005. A scalable parallel Monte Carlo method for free energy simulations of molecular systems. *J. Comput. Chem.* 26:72–77
37. Virnau P, Muller M. 2004. Calculation of free energy through successive umbrella sampling. *J. Chem. Phys.* 120:10925–30
38. Ensing B, De Vivo M, Liu ZW, Moore P, Klein ML. 2006. Metadynamics as a tool for exploring free energy landscapes of chemical reactions. *Acc. Chem. Res.* 39:73–81
39. Lelievre T, Rousset M, Stoltz G. 2007. Computation of free energy profiles with parallel adaptive dynamics. *J. Chem. Phys.* 126:134111
40. Babin V, Roland C, Sagui C. 2008. Adaptively biased molecular dynamics for free energy calculations. *J. Chem. Phys.* 128:134101
41. Babin V, Karpusenka V, Moradi M, Roland C, Sagui C. 2009. Adaptively biased molecular dynamics: an umbrella sampling method with a time-dependent potential. *Int. J. Quantum Chem.* 109:3666–78
42. Vanden-Eijnden E. 2009. Some recent techniques for free energy calculations. *J. Comput. Chem.* 30:1737–47
43. Knight JL, Brooks CL 3rd. 2009. λ-Dynamics free energy simulation methods. *J. Comput. Chem.* 30:1692–700
44. Dickson BM, Legoll F, Lelievre T, Stoltz G, Fleurat-Lessard P. 2010. Free energy calculations: an efficient adaptive biasing potential method. *J. Phys. Chem. B* 114:5823–30
45. Christ CD, Mark AE, van Gunsteren WF. 2010. Basic ingredients of free energy calculations: a review. *J. Comput. Chem.* 31:1569–82
46. Atchade YF, Liu JS. 2010. The Wang-Landau algorithm in general state spaces: applications and convergence analysis. *Stat. Sin.* 20:209–33

47. Kästner J. 2011. Umbrella sampling. *Wiley Interdiscip. Rev. Comput. Mol. Sci.* 1:932–42
48. Pratt LR. 1986. A statistical method for identifying transition states in high dimensional problems. *J. Chem. Phys.* 85:5045–48
49. Yan QL, Faller R, de Pablo JJ. 2002. Density-of-states Monte Carlo method for simulation of fluids. *J. Chem. Phys.* 116:8745–49
50. Faller R, de Pablo JJ. 2003. Density of states of a binary Lennard-Jones glass. *J. Chem. Phys.* 119:4405–408
51. Kim EB, Guzmán O, Grollau S, Abbott NL, de Pablo JJ. 2004. Interactions between spherical colloids mediated by a liquid crystal: a molecular simulation and mesoscale study. *J. Chem. Phys.* 121:1949–61
52. Mastny EA, de Pablo JJ. 2005. Direct calculation of solid-liquid equilibria from density-of-states Monte Carlo simulations. *J. Chem. Phys.* 122:124109
53. Jayasri D, Sastry VSS, Murthy KPN. 2005. Wang-Landau Monte Carlo simulation of isotropic-nematic transition in liquid crystals. *Phys. Rev. E* 72:036702
54. Chopra M, Müller M, de Pablo JJ. 2006. Order-parameter-based Monte Carlo simulation of crystallization. *J. Chem. Phys.* 124:134102
55. Poulain P, Calvo F, Antoine R, Broyer M, Dugourd P. 2006. Performances of Wang-Landau algorithms for continuous systems. *Phys. Rev. E* 73:056704
56. Zhou CG, Schulthess TC, Torbrugge S, Landau DP. 2006. Wang-Landau algorithm for continuous models and joint density of states. *Phys. Rev. Lett.* 96:120201
57. Seaton DT, Mitchell SJ, Landau DP. 2008. Developments in Wang-Landau simulations of a simple continuous homopolymer. *Braz. J. Phys.* 38:48–53
58. Ghosh J, Faller R. 2008. Comparing the density of states of binary Lennard-Jones glasses in bulk and film. *J. Chem. Phys.* 128:124509
59. Jain TS, de Pablo JJ. 2002. A biased Monte Carlo technique for calculation of the density of states of polymer films. *J. Chem. Phys.* 116:7238–43
60. Gront D, Kolinski A, Skolnick J. 2000. Comparison of three Monte Carlo conformational search strategies for a proteinlike homopolymer model: folding thermodynamics and identification of low-energy structures. *J. Chem. Phys.* 113:5065–71
61. Fenwick MK, Escobedo FA. 2003. Expanded ensemble and replica exchange methods for simulation of protein-like systems. *J. Chem. Phys.* 119:11998–2010
62. Rathore N, Knotts TA, de Pablo JJ. 2003. Configurational temperature density of states simulations of proteins. *Biophys. J.* 85:3963–68
63. Rathore N, Knotts TA, de Pablo JJ. 2003. Density of states simulations of proteins. *J. Chem. Phys.* 118:4285–90
64. Nagasima T, Kinjo AR, Mitsui T, Nishikawa K. 2007. Wang-Landau molecular dynamics technique to search for low-energy conformational space of proteins. *Phys. Rev. E* 75:066706
65. Swetnam AD, Allen MP. 2011. Improving the Wang-Landau algorithm for polymers and proteins. *J. Comput. Chem.* 32:816–21
66. Plimpton S. 1995. Fast parallel algorithms for short-range molecular dynamics. *J. Comput. Phys.* 117:1–19
67. Phillips JC, Braun R, Wang W, Gumbart J, Tajkhorshid E, et al. 2005. Scalable molecular dynamics with NAMD. *J. Comput. Chem.* 26:1781–802
68. Case DA, Cheatham TE, Darden T, Gohlke H, Luo R, et al. 2005. The Amber biomolecular simulation programs. *J. Comput. Chem.* 26:1668–88
69. Hess B, Kutzner C, van der Spoel D, Lindahl E. 2008. GROMACS 4: algorithms for highly efficient, load-balanced, and scalable molecular simulation. *J. Chem. Theory Comput.* 4:435–47
70. Brooks BR, Brooks CL 3rd, Mackerell AD Jr, J, Nilsson L, Petrella RJ, et al. 2009. CHARMM: the biomolecular simulation program. *J. Comput. Chem.* 30:1545–614
71. Harvey MJ, Giupponi G, Fabritiis GD. 2009. ACEMD: accelerating biomolecular dynamics in the microsecond time scale. *J. Chem. Theory Comput.* 5:1632–39
72. Marsili S, Barducci A, Chelli R, Procacci P, Schettino V. 2006. Self-healing umbrella sampling: a non-equilibrium approach for quantitative free energy calculations. *J. Phys. Chem. B* 110:14011–13
73. Laio A, Parrinello M. 2002. Escaping free-energy minima. *Proc. Natl. Acad. Sci. USA* 99:12562–66
74. Micheletti C, Laio A, Parrinello M. 2004. Reconstructing the density of states by history-dependent metadynamics. *Phys. Rev. Lett.* 92:170601

75. Laio A, Gervasio FL. 2008. Metadynamics: a method to simulate rare events and reconstruct the free energy in biophysics, chemistry and material science. *Rep. Prog. Phys.* 71:126601
76. Min DH, Liu YS, Carbone I, Yang W. 2007. On the convergence improvement in the metadynamics simulations: a Wang-Landau recursion approach. *J. Chem. Phys.* 126:194104
77. Metropolis N, Rosenbluth AW, Rosenbluth MN, Teller AH, Teller E. 1953. Equation of state calculations by fast computing machines. *J. Chem. Phys.* 21:1087–92
78. Morozov AN, Lin SH. 2007. Accuracy and convergence of the Wang-Landau sampling algorithm. *Phys. Rev. E* 76:026701
79. Zhou CG, Bhatt RN. 2005. Understanding and improving the Wang-Landau algorithm. *Phys. Rev. E* 72:025701
80. Earl DJ, Deem MW. 2005. Markov chains of infinite order and asymptotic satisfaction of balance: application to the adaptive integration method. *J. Phys. Chem. B* 109:6701–4
81. Yan Q, de Pablo JJ. 2003. Fast calculation of the density of states of a fluid by Monte Carlo simulations. *Phys. Rev. Lett.* 90:035701
82. Lee HK, Okabe Y, Landau DP. 2006. Convergence and refinement of the Wang-Landau algorithm. *Comput. Phys. Commun.* 175:36–40
83. Belardinelli RE, Pereyra VD. 2007. Fast algorithm to calculate density of states. *Phys. Rev. E* 75:046701
84. Belardinelli RE, Manzi S, Pereyra VD. 2008. Analysis of the convergence of the 1/*t* and Wang-Landau algorithms in the calculation of multidimensional integrals. *Phys. Rev. E* 78:067701
85. Zhou C, Su J. 2008. Optimal modification factor and convergence of the Wang-Landau algorithm. *Phys. Rev. E* 78:046705
86. de Pablo JJ, Laso M, Suter UW. 1992. Simulation of polyethylene above and below the melting point. *J. Chem. Phys.* 96:2395–403
87. Siepmann JI, Frenkel D. 1992. Configurational bias Monte Carlo: a new sampling scheme for flexible chains. *Mol. Phys.* 75:59–70
88. Dijkstra M, Frenkel D, Hansen JP. 1994. Phase separation in binary hard-core mixtures. *J. Chem. Phys.* 101:3179–89
89. Butler BD, Ayton O, Jepps OG, Evans DJ. 1998. Configurational temperature: verification of Monte Carlo simulations. *J. Chem. Phys.* 109:6519–22
90. Yan QL, Jain TS, de Pablo JJ. 2004. Density-of-states Monte Carlo simulation of a binary glass. *Phys. Rev. Lett.* 92:235701
91. Dayal P, Trebst S, Wessel S, Wurtz D, Troyer M, et al. 2004. Performance limitations of flat-histogram methods. *Phys. Rev. Lett.* 92:097201
92. Shell MS, Debenedetti PG, Panagiotopoulos AZ. 2004. Flat-histogram dynamics and optimization in density of states simulations of fluids. *J. Phys. Chem. B* 108:19748–55
93. Troster A, Dellago C. 2005. Wang-Landau sampling with self-adaptive range. *Phys. Rev. E* 71:066705
94. Cunha-Netto AG, Caparica AA, Tsai SH, Dickman R, Landau DP. 2008. Improving Wang-Landau sampling with adaptive windows. *Phys. Rev. E* 78:055701
95. Zhan L. 2008. A parallel implementation of the Wang-Landau algorithm. *Comput. Phys. Commun.* 179:339–44
96. Janosi L, Doxastakis M. 2009. Accelerating flat-histogram methods for potential of mean force calculations. *J. Chem. Phys.* 131:054105
97. Trebst S, Huse DA, Troyer M. 2004. Optimizing the ensemble for equilibration in broad-histogram Monte Carlo simulations. *Phys. Rev. E* 70:046701
98. Escobedo FA, Martínez-Veracoechea FJ. 2007. Optimized expanded ensembles for simulations involving molecular insertions and deletions. I. Closed systems. *J. Chem. Phys.* 127:174103
99. Martínez-Veracoechea FJ, Escobedo FA. 2008. Variance minimization of free energy estimates from optimized expanded ensembles. *J. Phys. Chem. B* 112:8120–28
100. Frenkel D. 2004. Speed-up of Monte Carlo simulations by sampling of rejected states. *Proc. Natl. Acad. Sci. USA* 101:17571–75
101. Chopra M, de Pablo JJ. 2006. Improved density of states Monte Carlo method based on recycling of rejected states. *J. Chem. Phys.* 124:114102

102. Shell MS, Debenedetti PG, Panagiotopoulos AZ. 2003. An improved Monte Carlo method for direct calculation of the density of states. *J. Chem. Phys.* 119:9406–11
103. Wu Y, Schmitt JD, Car R. 2004. Mapping potential energy surfaces. *J. Chem. Phys.* 121:1193–200
104. Gervasio FL, Laio A, Parrinello M. 2005. Flexible docking in solution using metadynamics. *J. Am. Chem. Soc.* 127:2600–7
105. Ensing B, Klein ML. 2005. Perspective on the reactions between F^- and CH_3CH_2F: the free energy landscape of the E2 and S_N2 reaction channels. *Proc. Natl. Acad. Sci. USA* 102:6755–59
106. Babin V, Roland C, Darden TA, Sagui C. 2006. The free energy landscape of small peptides as obtained from metadynamics with umbrella sampling corrections. *J. Chem. Phys.* 125:204909
107. Singh S, Chiu C-c, de Pablo J. 2011. Flux tempered metadynamics. *J. Stat. Phys.* 144:1–14
108. Bussi G, Laio A, Parrinello M. 2006. Equilibrium free energies from nonequilibrium metadynamics. *Phys. Rev. Lett.* 96:090601
109. Crespo Y, Marinelli F, Pietrucci F, Laio A. 2010. Metadynamics convergence law in a multidimensional system. *Phys. Rev. E* 81:055701
110. Barducci A, Bussi G, Parrinello M. 2008. Well-tempered metadynamics: a smoothly converging and tunable free-energy method. *Phys. Rev. Lett.* 100:020603
111. Li H, Min D, Liu Y, Yang W. 2007. Essential energy space random walk via energy space metadynamics method to accelerate molecular dynamics simulations. *J. Chem. Phys.* 127:094101
112. Zhang Y, Voth GA. 2011. Combined metadynamics and umbrella sampling method for the calculation of ion permeation free energy profiles. *J. Chem. Theory Comput.* 7:2277–83
113. Kumar S, Bouzida D, Swendsen RH, Kollman PA, Rosenberg JM. 1992. The weighted histogram analysis method for free-energy calculations on biomolecules. 1. The method. *J. Comput. Chem.* 13:1011–21
114. Kumar S, Rosenberg JM, Bouzida D, Swendsen RH, Kollman PA. 1995. Multidimensional free-energy calculations using the weighted histogram analysis method. *J. Comput. Chem.* 16:1339–50
115. Laio A, Rodriguez-Fortea A, Gervasio FL, Ceccarelli M, Parrinello M. 2005. Assessing the accuracy of metadynamics. *J. Phys. Chem. B* 109:6714–21
116. Raiteri P, Laio A, Gervasio FL, Micheletti C, Parrinello M. 2006. Efficient reconstruction of complex free energy landscapes by multiple walkers metadynamics. *J. Phys. Chem. B* 110:3533–39
117. Faller R, Yan QL, de Pablo JJ. 2002. Multicanonical parallel tempering. *J. Chem. Phys.* 116:5419–23
118. Rosta E, Hummer G. 2009. Error and efficiency of replica exchange molecular dynamics simulations. *J. Chem. Phys.* 131:165102
119. Bussi G, Gervasio FL, Laio A, Parrinello M. 2006. Free-energy landscape for β hairpin folding from combined parallel tempering and metadynamics. *J. Am. Chem. Soc.* 128:13435–41
120. Piana S, Laio A. 2007. A bias-exchange approach to protein folding. *J. Phys. Chem. B* 111:4553–59
121. Kannan S, Zacharias M. 2010. Application of biasing-potential replica-exchange simulations for loop modeling and refinement of proteins in explicit solvent. *Proteins Struct. Funct. Bioinforma.* 78:2809–19
122. Smiatek J, Heuer A. 2011. Calculation of free energy landscapes: a histogram reweighted metadynamics approach. *J. Comput. Chem.* 32:2084–96
123. Tribello GA, Ceriotti M, Parrinello M. 2010. A self-learning algorithm for biased molecular dynamics. *Proc. Natl. Acad. Sci. USA* 107:17509–14
124. Bonomi M, Branduardi D, Bussi G, Camilloni C, Provasi D, et al. 2009. PLUMED: a portable plugin for free-energy calculations with molecular dynamics. *Comput. Phys. Commun.* 180:1961–72

Annual Review of Chemical and Biomolecular Engineering

Volume 3, 2012

Contents

Indexes

Errata

An online log of corrections to *Annual Review of Chemical and Biomolecular Engineering* articles may be found at http://chembioeng.annualreviews.org/errata.shtml